Experimental investigation of the lattice and electronic temperatures in $Ga_{0.47}In_{0.53}As/Al_{0.62}Ga_{0.38}As_{1-x}Sb_x$ quantum-cascade lasers

Miriam S. Vitiello[a] and Gaetano Scamarcio[b]
CNR-INFM Regional Laboratory LIT[3], Dipartimento Interateneo di Fisica "M. Merlin," Università degli Studi di Bari, Via Amendola 173, 70126 Bari, Italy

Vincenzo Spagnolo
CNR-INFM Regional Laboratory LIT[3], Dipartimento Interateneo di Fisica "M. Merlin," Politecnico di Bari, Via Amendola 173, 70126 Bari, Italy

Antonia Lops
CNR-INFM Regional Laboratory LIT[3], Dipartimento Interateneo di Fisica "M. Merlin," Università degli Studi di Bari, Via Amendola 173, 70126 Bari, Italy

Quankui Yang, Christian Manz, and Joachim Wagner
Fraunhofer Institute for Applied Solid State Physics (IAF), Tullastrasse 72, D-79108 Freiburg, Germany

(Received 11 October 2006; accepted 21 February 2007; published online 20 March 2007)

The authors extracted the thermal resistance (R_L=9.6 K/W) and the electrical power dependence of the electronic temperature (R_e=12.5 K/W) of $Ga_{0.47}In_{0.53}As/Al_{0.62}Ga_{0.38}As_{1-x}Sb_x$ quantum-cascade lasers (QCLs) operating at 4.9 μm, in the lattice temperature range of 60–90 K. The low electron-lattice coupling constant α=10.4 K cm^2/kA can be related to the beneficial effect of the high conduction band offset, peculiar to the GaInAs/AlGaAsSb material system, on the electron leakage. The authors found an active region cross-plane thermal conductivity value $k_\perp$=1.8±0.1 W/(K m), which is approximately three times larger than that measured in QCLs with GaInAs/AlInAs heterostructures. © *2007 American Institute of Physics*. [DOI: 10.1063/1.2717018]

There is actually considerable interest to extend the operation of quantum-cascade lasers (QCLs) in the 3–5 μm band. The absorption lines of many important chemical compounds fall in this spectral region. However, the operation of GaInAs/AlInAs QCLs at shorter wavelengths is limited by the available range of intersubband transition energies, typically ~50% of the conduction band energy discontinuity. Laser action in the range of 3–4.3 μm has been achieved by using lattice-matched GaInAs/AlAsSb (Refs. 1 and 2) and $Ga_{0.47}In_{0.53}As/Al_{0.62}Ga_{0.38}As_{1-x}Sb_x$ quaternary alloy heterostructures.[3]

Recently, we have shown that in GaInAs/AlAsSb-based QCLs, the interface configuration and the related band alignment are strongly sample dependent, due to the high sensitivity of the layer and interface quality to the growth procedure.[4] In this letter, we report on the simultaneous determination of the electronic and lattice temperatures as a function of the electrical power (P) in $Ga_{0.47}In_{0.53}As/Al_{0.62}Ga_{0.38}As_{1-x}Sb_x$ QCLs operating at 4.9 μm.[3] In previous studies, we have experimentally assessed the thermal and nonequilibrium electronic properties in GaAs- and GaInAs-based QCLs.[5–7] However, such an important piece of information is still lacking in Sb-based QCLs.

The layer sequence in the active region of the investigated device and the calculated conduction and valence band structures are shown in Fig. 1.[8] Twenty-five periods of alternating active regions and injection regions were sandwiched between two 400 nm thick GaInAs layers n doped to $n=1\times10^{17}$ cm^{-3}. The layer sequence was grown by molecular beam epitaxy (MBE) without growth interruption on an S-doped n-InP (001) substrate. After MBE growth, the sample was transferred into a metal-organic vapor phase epitaxy system to grow Si-doped InP layers ($n=5\times10^{17}$ cm^{-3}, 20 nm; 2×10^{17} cm^{-3}, 1300 nm; and 7×10^{18} cm^{-3}, 1300 nm), serving as the upper waveguide cladding and contact layers. The InP substrate acts as a lower waveguide cladding. Ridge waveguides 10 μm wide were defined using

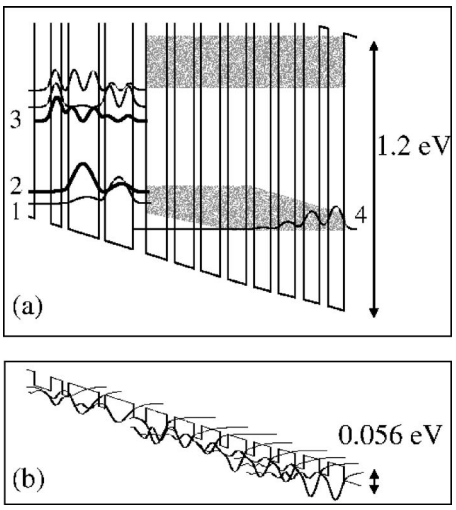

FIG. 1. (a) Conduction and (b) valence band structures of one period of the active region calculated with a voltage drop of 400 mV per stage using a self-consistent method based on the iterative solution of the Schrödinger and Poisson coupled equations. Beginning with the leftmost injection barrier, the layer thicknesses measured in nm are **2.5**/1.7/**1.0**/4.6/**1.0**/4.3/**2.0**/3.2/**1.1**/3.0/**1.1**/2.9/**1.2**/2.7/**1.2**/2.6/**1.2**/2.5/**1.3**/2.4/**1.4**/2.4. The numbers in bold refer to barrier layers. The underlined layers are doped to $n=2\times10^{17}$ cm^{-3}. The shaded areas show the injector minibands.

[a]Electronic mail: vitiello@fisica.uniba.it
[b]Electronic mail: scamarcio@fisica.uniba.it

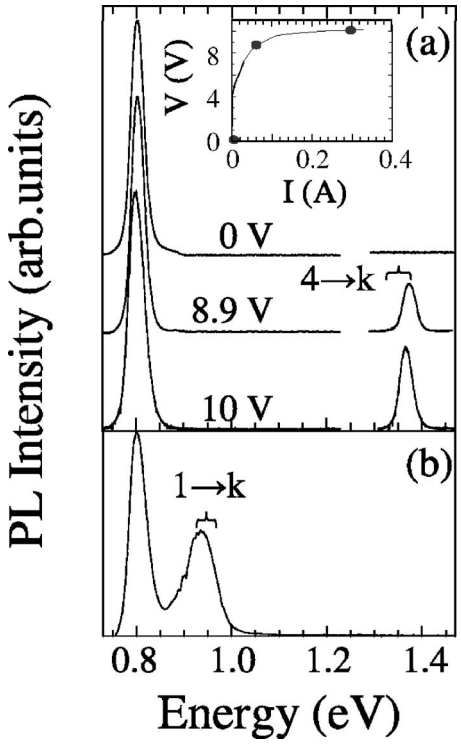

FIG. 2. (a): PL spectra measured at different applied voltages: 0, 8.9, and 10 V, as marked on the current-voltage characteristics shown in the inset. The heat sink temperature is T_H=60 K. The PL intensity in the range of 1.3–1.4 eV has been multiplied by a factor of 5. (b) PL spectrum measured from the (001) surface of an unprocessed sample in which the whole sequence of InP upper layers and ~200 nm of the InGaAs upper cladding have been removed by wet etching. The energy ranges of the transitions $4\rightarrow k$ and $1\rightarrow k$ between the conduction (j) and valence (k) subbands, calculated by varying the chemical composition (x) of the $Al_{0.62}Ga_{0.38}As_{1-x}Sb_x$ barrier and the conduction and valence band offsets by ~15%, are marked on the figures.

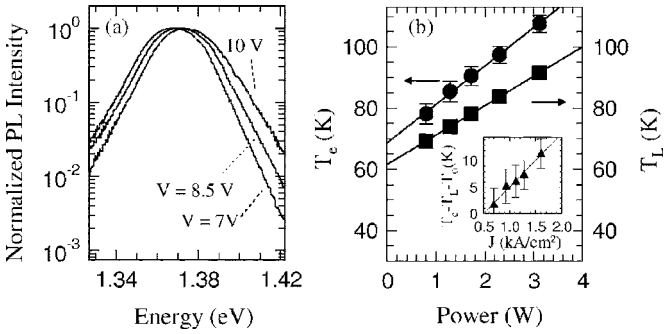

FIG. 3. (a) Voltage dependence of the $4\rightarrow k$ photoluminescence band, collected at the heat sink temperature T_H=60 K. (b) Electrical power dependence of the lattice temperature (■) and electronic temperature T_e of the subband j=4 (●) measured in the center of the active region on the QCL front facet at T_H=60 K. The lines are linear fits to the data. The extrapolated value of the temperature at P=0 W is due to the heating induced by the Kr^+ probe laser. Inset: Electronic temperature increase as a function of the current density measured at T_H=60 K. T_0=6.8 K is the constant temperature shift due to the Kr^+ laser heating.

photolithography and chemically assisted ion-beam etching. Subsequently, a 350 nm thick silicon nitride insulation layer was deposited, and windows were opened for top Ge/Ni/Au contact formation. Ti/Au layers have been then evaporated on the top of the ridges and under the substrate. Finally, the sidewalls and the top of the ridges have been covered with an electroplated 2.5 μm thick gold layer. Laser bars 1 mm long have been cleaved and epilayer-side mounted on copper mounts. This allowed to achieve laser action up to 400 K in pulsed mode and 73 K in continuous wave. A detailed description of the electrical and midinfrared optical characteristics is reported in Ref. 3.

Band-to-band photoluminescence (PL) experiments were carried out during device continuous wave operation. The devices were mounted on the cold finger of a helium-flow microcryostat. The heat sink temperature was kept at T_H=60 K, as measured by a Si diode mounted close to the device and controlled by an active feedback system, including an heater. The 647 nm line of a Kr^+ laser was focused to a 2.5 μm spot onto the laser front facet by using an optical power density of 10^3 W/cm^2. The PL signal was dispersed using a 0.46 m monochromator and detected with a GaInAs diode array detector cooled to 240 K.

Figure 2 shows a set of representative PL spectra measured at zero bias, at threshold for current injection, and in the full conduction regime, as marked on the current-voltage characteristic shown in the inset. For voltages in the range V=0–6 V, the PL spectra show a single band peaked at 0.802 eV, ascribed to the band-to-band transitions involving the upper GaInAs cladding layer. No evidence of signals associated with defect levels localized at the interfaces[4] is present in our spectra. Also, PL bands related to transitions involving the active region subbands are not visible. When current flows in the device, an additional band located at ~1.37 eV appears. This band redshifts at ~1.36 eV when the full conduction regime is reached ($V\approx$10 V), and its intensity increases with the injected current.

The absence of signals associated with the active region subbands at low voltages can be explained considering that the InP and the GaInAs layers embedding the active region core act as confinement ground state layers. To support this assumption, we have selectively etched the whole sequence of InP upper layers and ~200 nm of the GaInAs upper cladding from a small portion of the same unprocessed wafer. The PL spectrum collected under the same experimental conditions of the investigated lasers is reported in Fig. 2(b). While the signal coming from the GaInAs layer is still present, an additional PL band located at ~0.94 eV appears. In order to associate the measured structures with the relevant band-to-band transitions, we have compared our experimental results with band-structure calculations as a function of the applied voltage. Due to the uncertainty in the chemical composition of the quaternary barrier, we have varied the effective masses and the band-structure parameters, allowing for a 15% fluctuation of their nominal values. The comparison allows us to ascribe the band at 0.94 eV to $1\rightarrow k$ transitions (k denoting valence subbands). The PL band peaked at ~1.36–1.37 eV in Fig. 2(a) is ascribed to transitions involving the injector ground state (j=4), where the vast majority of electrons sit in the full conduction regime.[4] No features related to transitions starting from the upper laser level j=3 are visible in the investigated voltage range, reflecting a negligible relative population of level j=3 as compared with the ground injector level.

Figure 3(a) shows the voltage dependence of the $4\rightarrow k$ band. The peak energy of each band redshifts with P due to Joule heating. The exponential decay on the high energy side is proportional to $\exp[-E/k_BT_e]$, where T_e is the electronic temperature of the conduction subband j=4. Clearly, the

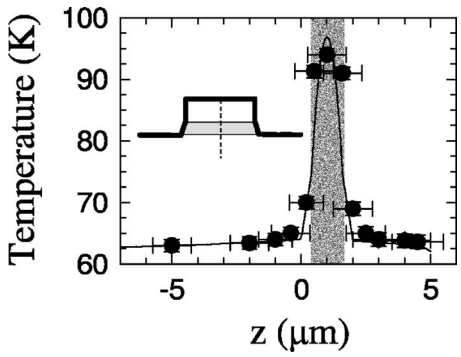

FIG. 4. Experimental (symbols) and calculated (solid line) temperature profiles measured along the growth axis in the center of the QCL front facet driven by a cw electrical power of 3.2 W, at T_H=60 K. The shaded area marks the active region layer.

electronic temperature of the ground state injector subband increases with P.

In order to extract the local temperature of the laser facet, which is a close estimate of the internal temperature in unipolar devices,[7] we have used the redshift of the PL peaks $1\rightarrow k$ and $4\rightarrow k$ of Fig. 2 as a thermometric property. A calibration curve has been obtained at zero current, measuring the shift of the band $1\rightarrow k$ as a function of T_H. Assuming that the energy of each subband scales equally with T_H and thus that the calibration curves of the PL bands $1\rightarrow k$ and $4\rightarrow k$ are rigidly shifted, we have compared the redshift of the band $4\rightarrow k$ with the measured calibration curve to extract the local lattice temperature (T_L).

The electronic and lattice temperatures T_e and T_L are plotted in Fig. 3(b) as a function of P. We found that the electronic temperature of the ground state injector subband j=4 increases linearly with P with a slope R_e=12.5 K/W, larger than the thermal resistance $R_L=dT_L/dP$=9.6 K/W. From the measured T_e and T_L values, we extracted the electron-lattice coupling constant $\alpha=(T_e-T_L)/J$ =10.4 K cm^2/kA. This value is significantly lower than that reported in GaAs/Al_xGa_{1-x}As mid-IR QCLs, where the value α=29.0 K cm^2/kA (α=44.7 K cm^2/kA) was measured for x=0.45 (x=1).[9] Low α values correspond to large electron-lattice coupling. The excellent electron-lattice coupling found for the structures investigated in the present work can be ascribed to the low electron leakage associated with the high (1.2 eV) conduction band offset,[9] peculiar to the GaInAs/AlGaAsSb material system.

To compare the thermal properties of Sb-based QCLs with devices based on different material systems, we have extracted the cross-plane component of the active region thermal conductivity ($k_\perp$), which mainly influences the device thermal resistance. Figure 4 shows the experimental facet temperature profile measured for P=3.2 W. The outcome of a two-dimensional steady state heat dissipation model has been fitted to the experimental data by leaving the anisotropic cross-plane thermal conductivity ($k_\perp$) as the only fitting parameter.[10,11] We found the value $k_\perp=1.8\pm0.1$ W/(K m) approximately three times larger than that measured at T_H=80 K in GaInAs/AlInAs [$k_\perp$=0.6 W/(K m)] mid-IR QCLs.[10] The above results can be explained considering the relation

$$(k_\perp)^{-1}=\left(\frac{d_a}{d_a+d_b}R_a+\frac{d_b}{d_a+d_b}R_b+\frac{N}{d_a+d_b}\mathrm{TBR}\right)$$

between $k_\perp$, the bulk resistivities of the materials ($R_{a,b}$), and the average thermal boundary resistance (TBR).[12] Here $d_{a,b}$ is the total thickness of GaInAs (a) and AlGaAsSb (b) layers in the active region and N is the total number of interfaces. Quaternary alloys are expected to have a lower thermal conductivity than ternary alloys,[12] but this has a negligible effect on the thermal conductivity of QCL's active regions. In fact, the latter is mostly determined by the high density of interfaces and hence by the third term in the above expression for $(k_\perp)^{-1}$. Theoretical calculations predict that the TBR of GaInAs/AlGaAsSb heterostructures at T_H=80 K is about a factor of 2 lower than that of GaInAs/AlInAs heterostructures,[12] due to the mismatch in the acoustic impedances and phonon densities of states.[12,13] Accordingly, the computed GaInAs/AlGaAsSb thermal conductivity value is ~2.5 times larger than that of GaInAs/AlInAs QCLs, in good agreement with our experimental results.

This work was partly supported by the European Project ANSWER (STRP 505642-1). The authors would like to thank Wolfgang Bronner and Klaus Köhler for their help in the fabrication of samples.

[1] Q. K. Yang, C. Manz, W. Bronner, Ch. Mann, L. Kirste, K. Köhler, and J. Wagner, Appl. Phys. Lett. **86**, 131107 (2005).
[2] D. G. Revin, J. W. Cockburn, M. J. Steer, R. J. Airey, M. Hopkinson, A. Krysa, L. R. Wilson, and S. Menzel, Appl. Phys. Lett. **90**, 021108 (2007).
[3] Q. K. Yang, C. Manz, W. Bronner, L. Kirste, K. Köhler, and J. Wagner, Appl. Phys. Lett. **86**, 131109 (2005).
[4] M. S. Vitiello, G. Scamarcio, V. Spagnolo, D. G. Revin, J. Cockburn, M. J. Steer, and R. J. Airey, J. Appl. Phys. **98**, 086107 (2005).
[5] V. Spagnolo, G. Scamarcio, H. Page, and C. Sirtori, Appl. Phys. Lett. **84**, 3690 (2004).
[6] M. S. Vitiello, G. Scamarcio, V. Spagnolo, B. S. Williams, S. Kumar, Q. Hu, and J. L. Reno, Appl. Phys. Lett. **86**, 111115 (2005).
[7] V. Spagnolo, M. Troccoli, G. Scamarcio, C. Gmachl, F. Capasso, A. Tredicucci, A. M. Sergent, A. L. Hutchinson, D. L. Sivco, and A. Y. Cho, Appl. Phys. Lett. **78**, 2095 (2001).
[8] We used a conduction band offset ΔE_C=1.2 eV, a valence band offset ΔE_V=0.056 eV, and a nonparabolicity coefficient $\gamma=1.13\times10^{-18}$ m^{-2}.
[9] V. Spagnolo, G. Scamarcio, W. Schrenk, and G. Strasser, Semicond. Sci. Technol. **19**, 1 (2004).
[10] A. Lops, V. Spagnolo, and G. Scamarcio, J. Appl. Phys. **100**, 043109 (2006).
[11] We used for the in-plane thermal conductivity the 75% of the weighted average of the thermal conductivities of the well and barrier materials. The following function (2890 T$^{-1.45}$)$\times10^2$ W/(K m) has been used for the heat conductivity of InP. This value is a factor of 0.84 lower for the layer doped at 2×10^{17} and of 0.72 for that doped at 7×10^{18}. For the Si_3N_4 insulating layer, the value k=15 W/(K m) has been used. The other parameters can be found in Ref. 10.
[12] C. Zhu, Y. Zhang, A. Li, and Z. Tian, J. Appl. Phys. **100**, 053105 (2006).
[13] R. J. Stoner and H. J. Maris, Phys. Rev. B **48**, 16373 (1993).